

Form Approved
OMB No. 0704-0188

1. REPORT DATE (DD-MM-YYYY)

Technical Papers

3. DATES COVERED (From - To)

4. TITLE AND SUBTITLE

5a. CONTRACT NUMBER	
---------------------	--

5b. GRANT NUMBER

5c. PROGRAM ELEMENT NUMBER	
----------------------------	--

6. AUTHOR(S)

5d. PROJECT NUMBER

1011

5e. TASK NUMBER

0046

5f. WORK UNIT NUMBER

3 46 204

7. PERFORMING ORGANIZATION NAME(S) AND ADDRESS(ES)

8. PERFORMING ORGANIZATION REPORT

Air Force Research Laboratory (AFMC)
AFRL/PRS
5 Pollux Drive
Edwards AFB CA 93524-7048

9. SPONSORING / MONITORING AGENCY NAME(S) AND ADDRESS(ES)

10. SPONSOR/MONITOR'S ACRONYM(S)

Air Force Research Laboratory (AFMC)
AFRL/PRS
5 Pollux Drive
Edwards AFB CA 93524-7048

11. SPONSOR/MONITOR'S
NUMBER(S)

Please see attached

12. DISTRIBUTION / AVAILABILITY STATEMENT

Approved for public release; distribution unlimited.

13. SUPPLEMENTARY NOTES

14. ABSTRACT

20030204 065

15. SUBJECT TERMS

16. SECURITY CLASSIFICATION OF:

17. LIMITATION OF ABSTRACT

18. NUMBER OF PAGES

19a. NAME OF RESPONSIBLE PERSON

Leilani Richardson

a. REPORT

b. ABSTRACT

c. THIS PAGE

Unclassified

Unclassified

Unclassified

19b. TELEPHONE NUMBER

TELEPHONE
(include area code)

(661) 275-5015

MEMORANDUM FOR PRS (In-House Publication)

FROM: PROI (STINFO)

21 February 2002

SUBJECT: Authorization for Release of Technical Information, Control Number: **AFRL-PR-ED-TP-2002-038**
C.W. Larson *et al.*, "Energy Conversion in Laser Propulsion III"

High-Power Laser Ablation 2002
(Taos, NM, 21-26 April 2002) (Deadline: 25 Mar 2002)

(Statement A)

1. This request has been reviewed by the Foreign Disclosure Office for: a.) appropriateness of distribution statement, b.) military/national critical technology, c.) export controls or distribution restrictions, d.) appropriateness for release to a foreign nation, and e.) technical sensitivity and/or economic sensitivity.

Comments: _____

Signature _____

Date _____

2. This request has been reviewed by the Public Affairs Office for: a.) appropriateness for public release and/or b.) possible higher headquarters review.

Comments: _____

Signature _____

Date _____

3. This request has been reviewed by the STINFO for: a.) changes if approved as amended, b.) appropriateness of references, if applicable; and c.) format and completion of meeting clearance form if required

Comments: _____

Signature _____

Date _____

4. This request has been reviewed by PR for: a.) technical accuracy, b.) appropriateness for audience, c.) appropriateness of distribution statement, d.) technical sensitivity and economic sensitivity, e.) military/national critical technology, and f.) data rights and patentability

Comments: _____

APPROVED/APPROVED AS AMENDED/DISAPPROVED

PHILIP A. KESSEL

Date

Technical Advisor

Space and Missile Propulsion Division

Energy Conversion in Laser Propulsion III

C. William Larson, Franklin B. Mead, Jr., and Wayne M. Kalliomaa

Propulsion Directorate

Air Force Research Laboratory

Edwards AFB, CA 93524-7680

Abstract

Conversion of pulses of CO₂ laser energy (18 microsecond pulses) to propellant kinetic energy was studied in a Myrabo Laser Lightcraft (MLL) operating with laser heated STP air and laser ablated delrin propellants. The MLL incorporates an inverted parabolic reflector that focuses laser energy into a toroidal volume where it is absorbed by a unit of propellant mass that is subsequently expanded in the geometry of the plug nozzle aerospike. With Delrin propellant, measurements of the coupling coefficients and the ablated mass as a function of laser pulse energy showed that the efficiency of conversion of laser energy to propellant kinetic energy was ~ 54%. With STP air, direct experimental measurement of efficiency was not possible because the propellant mass associated with measured coupling coefficients was not known. Thermodynamics predicted that the upper limit of the efficiency of conversion of the internal energy of laser heated air to jet kinetic energy, α , is ~ 0.30 for EQUILIBRIUM expansion to 1 bar pressure. For FROZEN expansion $\alpha \sim 0.27$. These upper limit efficiencies are nearly independent of the initial specific energy from 1 to 110 MJ/kg. With heating of air at its Mach 5 stagnation density (5.9 kg/m³ as compared to STP air density of 1.18 kg/m³) these efficiencies increase to about 0.55 (equilibrium) and 0.45 (frozen). Optimum blowdown from 1.18 kg/m³ to 1 bar occurs with expansion ratios ~ 1.5 to 4 as internal energy increases from 1 to 100 MJ/kg. Optimum expansion from the higher density state requires larger expansion ratios, 8 to 32. Expansion of laser ablated Delrin propellant appears to convert the absorbed laser energy more efficiently to jet kinetic energy because the effective density of the ablated gaseous Delrin is significantly greater than that of STP air.

NOMENCLATURE (in order of use)

E_f	kinetic energy of vehicle at end of mission.
m_f	mass of vehicle at end of mission.
v_f	velocity of vehicle at end of mission in inertial frame of reference.
η	efficiency of conversion of propellant kinetic energy to vehicle kinetic energy.
α	efficiency of conversion of propellant internal energy to propellant kinetic energy.
β	efficiency of absorption of laser energy by propellant.
γ	efficiency of transmission of ground based laser energy through atmosphere to vehicle.
E_L	laser energy per laser pulse.
v_e	exit velocity of propellant relative to the rocket, in the rocket frame of reference, m/s.
m	mass of rocket, kg.
F	Force or thrust of rocket, N = kg m/s ² .
t	time, s
ρ	propellant density, kg/m ³ .
$\langle v_e \rangle$	mass weighted average exit velocity of blowdown expansion in rocket frame of reference, m/s.
E_p	kinetic energy of propellant, J.
$\langle v_e^2 \rangle$	mass weighted average squared exit velocity of propellant in a blowdown expansion, m ² /s ² .
m_p	mass of propellant, kg.
I	impulse, Ns = kg m/s.
C	coupling coefficient, Ns/J or s/m.
Φ	ratio: $\langle v_e^2 \rangle / \langle v_e \rangle^2$.
C^*	normalized coupling coefficient, $C^* = C/\beta$.
v_e^*	normalized exit velocity, $v_e^* = \langle v_e \rangle / \Phi$.
$(u_e - u^0)^*$	normalized specific internal energy, $(u_e - u^0)^* = (u_e - u^0) / \Phi$.
u_e	specific internal energy of laser heated propellant, J/kg.
u^0	specific internal energy of propellant before laser heating, u^0_{air} at STP = -9.0×10^4 J/kg.

DISTRIBUTION STATEMENT A
Approved for Public Release
Distribution Unlimited

u_e	specific internal energy of propellant at the exit of the rocket after isentropic expansion.
V_{abs}	absorption volume.
V_{abs}^*	normalized absorption volume, $V_{abs}^* = V_{abs}/\beta$.
T	temperature, K.
P	pressure, bar.
h	specific enthalpy, J/kg.
s	specific entropy, J/kg K.
M_m	average molecular weight of a mixture, g/mole.
c_p	specific heat capacity at constant pressure.
v_a	velocity of sound, m/s.
$X(e^-)$	mole fraction of electrons.
ε	expansion ratio
A_e	area of exit surface
A_t	area of sonic surface or throat area

Subscripts, Acronyms, symbols

i	initial value of property
f	final value of property
c	property in chamber
t	property in throat
e	property in exit plane
p	property of propellant
MLL	Myrabo Laser Lightcraft
STP	Standard Temperature and Pressure, 298 K, 1.01326 bar

INTRODUCTION

Laser propulsion is limited by laser power, so optimization of the laser propulsion mission may be factored into optimization of four energy conversion efficiencies, which, in a first approximation, are independent of each other. In this idealization the kinetic energy of the propelled vehicle at the end of the mission may be expressed simply:

$$(1) \quad E_f = \frac{1}{2} m_f v_f^2 = \eta \alpha \beta \gamma E_L.$$

The "propulsion efficiency", η , is the efficiency with which jet kinetic energy is converted into vehicle kinetic energy. Sutton¹ pointed out, more than 50 years ago, that the instantaneous propulsion efficiency varies during a rocket mission and that it is unity only when the vehicle velocity in the inertial frame is equal to the jet velocity in the rocket frame. Unit propulsion efficiency is achieved when the jet is deposited as a stationary mass relative to an observer in the inertial frame of reference.

Then, 25-years ago, Moeckel² and Lo³ independently and nearly simultaneously published analyses of the optimization of laser rocket propulsion by maximizing η , and most recently, Phipps, Reilly and Campbell (2000, 2001)⁴ cited Moeckel's paper in their comprehensive analysis of the single stage, constant I_{sp} Earth to LEO rocket mission. They reiterated the fundamental limit that Newton's second law imposes: for rocket missions that start at zero initial velocity, the maximum η is 0.648, which is achieved when $f = 0.203$ and $v_f/v_e = 1.595$. For the Earth to LEO mission the effective "delta v" (v_f) is about 10 km/s, so the optimum single stage to orbit jet velocity is ~ 6.27 km/s, or specific impulse ~ 640 s.

In this paper we report a continuation of our previous work⁵ and analyze measurements of the overall efficiency of conversion of laser energy to propellant kinetic energy, $\alpha\beta$, based on various ballistic pendulum and flight experiments with Myrabo Laser Lightcraft, MLL [Messitt, Myrabo, and Mead (2000)⁶, Mead, Squires, Beairisto, and Thurston (2000)⁷]. The Phipps, et al.⁴ study defined an "ablation efficiency" and analyzed the Earth to LEO mission with unit ablation efficiency. Their ablation efficiency is equivalent to the product of α and β . Comparison of experimental results with thermodynamic analysis enables confining the range of permissible β that operates during the heating process. Wang's⁸ CFD plasma model of laser energy absorption by air have predicted plasma temperatures up to 30000 K with attendant low β values ~ 0.3 to 0.4 . It has been pointed out that β

approaches zero as the plasma temperature approaches $\sim 40,000$ K, where the plasma frequency approaches the laser frequency.^{8,9}

The Coupling Coefficient

Newton's second law expresses the thrust that results from expulsion of matter from a vehicle of mass m at velocity v_e as

$$(2) \quad F = -\frac{d(mv_e)}{dt},$$

where mv_e is the momentum of the jet exhaust in the vehicle frame of reference, [Corliss, (1960)]¹⁰. For the case where v_e is constant,

$$(3) \quad F = -v_e \frac{dm}{dt}.$$

Equation (2) may be used to define an average exit velocity for rockets where v_e is not constant, such as blowdown of a specified mass of hot propellant from a fixed volume, e.g., as in laser rockets and pulse detonation rockets:

$$(4) \quad \langle v_e \rangle = -\frac{\int_0^t F dt}{\int_{m_i}^{m_f} dm} = \frac{\int_{m_i}^{m_f} d(mv_e)}{\int_{m_i}^{m_f} dm} = \frac{\int_{\rho_i}^{\rho_f} d(\rho v_e)}{\int_{\rho_i}^{\rho_f} d\rho}.$$

so that $\langle v_e \rangle$ is the mass weighted average exit velocity and $F = -\langle v_e \rangle dm/dt$. Chemical thermodynamics may be used to rigorously establish an upper limit to $\langle v_e \rangle$ when the propellant equation of state is known and the initial and final states of the propellant expansion are specified.

The efficiency of conversion of laser energy to propellant kinetic energy, $\alpha\beta$, may be defined by energy conservation in terms of $\langle v_e^2 \rangle$ for the general case of variable v_e .

$$(5) \quad E_p = \frac{1}{2} m_p \langle v_e^2 \rangle = \alpha\beta E_L,$$

where the mass weighted average of the square of the propellant exit velocity is

$$(6) \quad \langle v_e^2 \rangle = \frac{\int_{\rho_i}^{\rho_f} d(\rho v_e^2)}{\int_{\rho_i}^{\rho_f} d\rho}.$$

The impulse, $I = \int F dt$, imparted to a test article by expansion of its propellant has been accurately measured with a ballistic pendulum in the past⁵. Momentum conservation requires equivalence between the measured impulse and the propellant impulse so that

$$(7) \quad I = m_p \langle v_e \rangle.$$

Thus, when I and m_p are both measured an experimental $\langle v_e \rangle$ may be obtained.

The momentum coupling coefficient, also a measured quantity, is the impulse imparted to a test article per unit laser energy incident on the propellant,

$$(8) \quad C = \frac{I}{E_L}.$$

Using the definitions embodied in Equations (5) - (8), C may be expressed in terms of α , β , $\langle v_e \rangle$, and $\langle v_e^2 \rangle$:

$$(9) \quad C = \frac{2\alpha\beta}{\langle v_e \rangle} \left[\frac{\langle v_e^2 \rangle}{\langle v_e^2 \rangle} \right] = \frac{2\alpha\beta\Phi}{\langle v_e \rangle}$$

If v_e is constant, $\Phi = \langle v_e^2 \rangle / \langle v_e^2 \rangle = 1$. Thermodynamics may be used to rigorously establish an upper limit to Φ and α for any specified free-expansion blowdown process when the propellant equation of state is known⁵. The Φ factor depends on the distribution of exit velocities, and is mathematically limited to $0.5 \leq \Phi \leq 1$. It has been shown^{5b} that Φ for optimum blowdown of laser heated air to 1 bar pressure increases from 0.95 at low specific energy (2 MJ/kg) to 0.98 at high specific energy (60 MJ/kg). The Φ factor arises in Equation (9) because the measured quantity, the jet impulse, is proportional to mass weighted average velocity whereas the jet kinetic energy is proportional to the mass weighted average of the squared velocity. Figure 1 shows the relationship between $C^* = C/\beta$, α , and $v_e^* = v_e / \Phi$. For a given α value, C^* decreases as $\langle v_e \rangle^*$ increases.

Isentropic conversion of internal energy of propellant to kinetic energy

Perfect isentropic conversion of internal energy to propellant kinetic energy occurs with no losses so that

$$(10) \quad \langle v_e^2 \rangle = 2\langle u_c - u_c^0 \rangle = 2\alpha(u_c - u^0), \text{ where}$$

$$(11) \quad \alpha = \langle u_c - u_c^0 \rangle / (u_c - u^0) = \langle v_e^2 \rangle / 2(u_c - u^0).$$

These definitions generate a second expression for C as a function of α that applies to isentropic energy conversion from initial states defined by $(u_c - u^0)$:

$$(12) \quad C = \beta [2\alpha\Phi / (u_c - u^0)]^{1/2}.$$

Figure 1 shows expansion isentropes in the $C^* - \alpha$ plane for various initial state values of $(u_c - u^0)^* = (u_c - u^0) / \Phi$ ranging from 1 MJ/kg to 110 MJ/kg. At constant α , C^* decreases as $(u_c - u^0)^*$ increases.

Experimental

Figure 2 shows a cross-section of the test article (MLL model 200-3/4) with a ring of Delrin installed in the shroud. The Delrin shown weighs ~ 10 g, occupies a volume of ~ 7 cm³, and has a surface area of ~ 25 cm². The exit area of the idealized plug-nozzle¹¹ is ~ 350 cm². Previous measurements⁵ of Delrin coupling coefficients as a function of laser pulse energy (18 μ s pulses) showed that they rise to a plateau of ~ 350 Ns/MJ above $E_L \sim 250$ J. At $E_L \sim 350$ J, the measured mass of ablated Delrin was ~ 40 mg, which is the mass of a uniform thin-film layer ~ 11 micrometers thick. Thus, from Equation (7) $v_e \sim 3100$ m/s and from Equation (9) $\alpha\beta\Phi \sim 0.54$. If $\beta = 1$, $C = C^*$, and Figure 1 shows that the initial specific internal energy that produces $\alpha = 0.54/\Phi$ (with $\Phi = 0.98$) in an isentropic expansion is $u_c - u^0 \sim 9$ MJ/kg. At the other extreme, if $\alpha\Phi = 1$, then $\beta = 0.54$, $C^* = 1.85 C$, and $u_c - u^0 \sim 4.8$ MJ/kg. By any analysis, these results show that Delrin is a remarkably efficient propellant for laser ablation propulsion.

For the case of air, the propellant mass m_p is unknown. Figure 2 may be used to visualize a reasonable absorption volume for the case where Delrin is absent and air is the heated material. The notion of an energy absorption volume, V_{abs} , may be invoked, which contains a mass of air propellant $m_p = \rho_c V_{abs}$ into which an amount of energy βE_L is deposited. In the limit where the time scale for energy absorption is much shorter than that for expansion, the propellant density within V_{abs} (the chamber) remains constant during energy absorption. This enables the initial specific internal energy of the propellant to be defined,

$$(13) \quad u_c - u^0 = \beta E_L / \rho_c V_{abs},$$

where $\rho_c = 1.18$ kg/m³ and $u^0 = -0.09 \times 10^6$ J/kg for air at STP. Table 1 provides a convenient list of values of the normalized absorption volume, $V_{abs}^* = V_{abs}/\beta$, derived from Equation (13) for values of $u_c - u^0$ and E_L that lie within the conceivable parameter space explored in experiments. Table 1 shows that an absorption volume for air, ~ 7 cm³,

would produce, with unit β and nominal E_L values between 100 and 400 J, heated air with internal energy between 10 and 40 MJ/kg. If the Delrin surface shown in the figure, about 25 cm², is a suitable representation of the sonic surface of expanding air, then, with an idealized plug-nozzle exit area¹¹ of ~ 350 cm², the expansion ratio in this test article may be as large as ~ 14. Previously reported experiments^{5a} showed that air coupling coefficients with a "loosely" focused laser increased to a plateau value of $C(\text{loose focus}) \sim 150$ Ns/MJ above $E_L \sim 150$ J. With a "tightly" focused laser they increased to a plateau value of $C(\text{tight focus}) \sim 100$ Ns/MJ above $E_L \sim 300$ J. As shown below, the maximum value of $\alpha\Phi$ for air in a chemical equilibrium isentropic expansion is $\alpha\Phi \sim 0.25$ and it is almost independent of initial specific internal energy and initial temperature. Table 2 summarizes the minimum values of β , $u_e - u^\circ$, C^* , and temperature for various reasonable values of V_{abs} and m_p . For $\beta = 1$, $m_p = 5.1$ mg (tight focus) or $m_p = 5.6$ mg (loose focus). These are the smallest values of m_p consistent with the measured C and E_L .

Air Mollier Diagram - Transformation of isentropes to the $C^* - \alpha$ plane

Figure 3 shows the chemical equilibrium Mollier diagram ($u-s$ plane) for air up to 24,000 K. Figure 3 is based on the database maintained at NASA/Glenn [McBride and Gordon (1996)]¹², which is certified accurate up to 20,000 K and which is based on extended 9-parameter fits to enthalpy, heat capacity, and entropy of neutral species and singly charged ions. Above 20,000 K doubly charged ions begin to contribute but these are not included in the database. This limitation leads to predictions of temperatures (at specified u and p) that are too high for plasmas above ~ 20,000 K.

Figure 4 shows a series of isentropes (vertical lines) on the Mollier diagram. These are representations of equilibrium isentropic expansions that originate from initial states located along the constant density line, $\rho = 1.18$ kg/m³, and specific internal energies ranging from 1 to 100 MJ/kg. Table 3 summarizes other interesting thermodynamic properties under conditions of chemical equilibrium: T , P , h , s , M_m , c_p , v_a , c_p/c_v , and $X(\epsilon)$. Table 4 provides properties of Mach 5 air at its stagnation density¹³, 5.9 kg/m³. Since the entropy of the initial and final states are equal, the thermodynamic state of the propellant in the exit surface is uniquely defined when only one additional property in the exit surface is specified, such as the exit pressure or the expansion ratio, which are also indicated in Figure 4. The expansion ratio, ϵ , is the ratio of the area of the exit surface to the area of the sonic surface or nozzle throat, and for isentropic expansions this may be represented in terms of thermodynamic properties in the nozzle throat and exit plane: $\epsilon = A_e/A_t = \rho_t v_t / \rho_e v_e$.

Figure 5 shows transformations of the isentropes in the Mollier plane to the $C^* - \alpha$ plane for equilibrium expansions from an initial density of STP air, 1.18 kg/m³. Lines of constant ϵ and ρ_e are almost exactly coincident. Lines of constant exit pressure run nearly parallel to lines of constant ϵ and ρ_e , and all are nearly vertical, indicating that α is nearly independent of v_e and $u_e - u^\circ$. At five times higher density, the constant exit pressure lines are nearly coincident with the STP constant pressure lines but their exit pressures are about five times higher. Thus, in the $C^* - \alpha$ plane, the 0.2 atm exit pressure line at $\rho_e = 1.18$ kg/m³ is almost coincident with a 1 atm exit pressure line at $\rho_e = 5.90$ kg/m³. The effect of higher ρ_e is to increase α from ~ 0.4 to 0.6.

DISCUSSION

Coupling coefficients measured with the Figure 2 test model were reported in our previous papers⁵. With increasing laser energy they rise to plateaus above about 300 J. At $E_L \sim 350$ J, $C(\text{Delrin}) \sim 350$ Ns/MJ and the ablated/vaporized mass was $m_p \sim 40$ mg. This means that $\langle v_e \rangle \sim 3100$ m/s by Equations (7) and (8), and $\alpha\beta\Phi \sim 0.54$ by Equation (9). Thus, since $\beta\Phi < 1$, $\alpha > 0.54$, which is remarkably high. Air and Delrin will show very similar expansion behavior. As shown previously^{5b}, the dependence of α on the density of the heated air is quite strong. At $[u_e - u^\circ]^* = 10$ MJ/kg and expansion to 1 bar, the instantaneous α increases from about 0.43 to about 0.60 when the density increases from the STP value (1.18 kg/m³) to its Mach 5 stagnation value (5.9 kg/m³). These instantaneous α values decrease to about 0.32 and 0.50 respectively for the free-expansion blowdown process^{5b}. An α value around 0.5 is reasonable when the density of the ablated and vaporized Delrin is as high as ~ 6 kg/m³ and the blowdown expansion is near perfect with $\epsilon \sim 16$. Most importantly, it appears that most of the inefficiency in the composite $\alpha\beta\Phi$ efficiency is carried by $\alpha\Phi$ and that β is very close to unity.

Coupling coefficients for air were found to depend strongly on the quality of the laser beam, as between a tightly focused beam that produced a lower $C \sim 100$ Ns/MJ than a loosely focused beam, which produced $C \sim 150$ Ns/MJ. This may be due to the tight beam heating a smaller mass of air to a higher energy than the more diffuse loosely focused beam. Although the exit velocity would be higher in the tight beam case, the total impulse may be

lower because the heated mass is lower. Figure 2 shows the geometry and size relationship of a 7 cm³ absorption volume inside the shroud, which contains ~ 8 mg of air. With $C(\text{air, loose focus}) = 150 \text{ Ns/MJ}$ at $E_L = 300 \text{ J}$, and $m_p = 8 \text{ mg}$ we may deduce $\langle v_e \rangle \sim 5600 \text{ m/s}$, and $\alpha\beta\Phi \sim 0.42$. If the absorption volume is double, then $\langle v_e \rangle$ and $\alpha\beta\Phi$ are halved. Figure 5 shows that STP air heated to 10 MJ/kg for example would blowdown to 1 bar with $\alpha = 0.32$ (equilibrium expansion) or $\alpha = 0.27$ (frozen expansion).

If we accept that a reasonable upper limit operational alpha is ~ 0.30 in our experiments $\alpha < 0.3$, then the measured $C \sim 150 \text{ Ns/MJ}$ and Equations (7-9) with $\beta\Phi = 1$ require $\langle v_e \rangle < 4000 \text{ m/s}$, and $m_p > 11 \text{ mg}$. Now if $\beta\Phi$ is ~ 0.3 as has been suggested by CFD modeling,⁸ then the upper limit of $\langle v_e \rangle$ decreases to 1200 m/s and the lower limit of m_p increases to 36 mg. It would seem apparent that the value of β is somewhat larger than 0.3 because both the upper limit $\langle v_e \rangle$ and lower limit m_p with $\beta = 0.3$ are not reasonable for the geometry shown in Figure 2.

CONCLUSIONS

Experimental studies of the propulsion of a 200-3/4 model Myrabo Laser Lightcraft heated by 10.6 μ radiation from a CO₂ laser showed that the efficiency of conversion of laser energy to propellant kinetic energy was 54% for Debrin propellant.

Thermodynamic analysis of isentropic expansion of a unit mass of air after laser heating at constant volume was examined under conditions where either chemical equilibrium or frozen composition was maintained. The upper limit for the efficiency of conversion of internal to kinetic energy in optimum blowdown to 1 bar pressure is $\alpha \sim 0.25$, which is nearly independent of the initial energy. For STP air, blowdown to 1 bar is achieved with expansion ratios from $\epsilon \sim 4$ at high energy to $\epsilon \sim 8$ at low energy. With this small effective $\epsilon \sim 4$, equilibrium expansion was only slightly more efficient than frozen expansion. Heating of propellant to higher energy states resulted in only slightly lower α but much higher exit velocity. The thermodynamic limitations were illustrated by process representations of blowdown in the Mollier plane.

REFERENCES

1. Sutton, George P., "Rocket Propulsion Elements, An Introduction to the Engineering of Rockets," (John Wiley and Sons, Inc., copyright 1949), page 17. See also: Sutton, George P., and Biblarz, Oscar, "Rocket Propulsion Elements, Seventh Edition," (John Wiley and Sons, Inc., New York, copyright 2001). page 38.
2. Moeckel, W. E., "Optimum exhaust velocity for laser-driven rockets," J. Spacecraft, Vol. 12, No. 11, Pages 700-701, manuscript received May 12, 1975, revision received July 11, 1975.
3. Lo, R. E., "Propulsion by laser energy transmission (considerations to selected problems)," IAF PAPER 76-165, October 1, 1976, 11 pages.
4. Phipps, C. R., Reilly, J. P., and Campbell, J. W., "Optimum parameters for laser-launching objects into low earth orbit," *Lasers and Particle Beams*, 18(1), (2001), pp 1-35. See also: Phipps, C. R., Reilly, J. P., and Campbell, J. W., "Laser launching a 5-kg object into low earth orbit," Presented at the Third International Symposium on High Power Laser Ablation, Santa Fe, NM, 23-28 April 2000, *Proceedings of SPIE* 4065, 502 (2000).
5. (a) Larson, C. W., and Mead, F. B. Jr., "Energy Conversion in Laser Propulsion," 39th AIAA Aerospace Sciences Meeting, 8-11 January 2001, Reno, NV, Paper No. 2001-0646, (b) Larson, C. W., Mead, F. B. Jr., and Kalliomaa, W. M., "Energy Conversion in Laser Propulsion II" 40th AIAA Aerospace Sciences Meeting, 14-17 January 2002, Reno, NV, Paper No. 2002-0632.
6. Messitt, Donald G., Myrabo, Leik N. and Mead, Franklin B. Jr., "Laser initiated blast wave for launch vehicle propulsion," 36th AIAA Joint Propulsion Conference, 16-19 July 2000, Huntsville, AL, paper 2000-3035.
7. Mead, Franklin B. Jr., Squires, Stephen, Beairst, Chris, and Thurston, Mike, "Flights of a laser-powered Lightcraft during laser beam hand-off experiments," 36th AIAA Joint Propulsion Conference, 16-19 July 2000, Huntsville, AL, paper 2000-3484.
8. (a) Wang, Ten-See, Mead, Franklin B. Jr., and Larson, Carl W., "Analysis of the Effect of Pulse Width on Laser Lightcraft Performance," 37th AIAA Joint Propulsion Conference, 8-11 July 2001, Salt Lake City, UT, Paper No. 2001-3664. See also: (b) Liu, Jiwen, Chen, Yen-Sen, and Wang, Ten-See, "Accurate prediction of radiative heat transfer in laser induced air plasmas," 34th AIAA Thermophysics Conference, 19-22 June 2000, Denver, CO, paper 2000-2370. See also (c) Wang, Ten-See, Chen, Yen-Sen, Liu, Jiwen, Myrabo, Leik N., and Mead, Franklin B. Jr., "Advanced Performance Modeling of Experimental Laser Lightcrafts," 39th AIAA Aerospace Sciences Meeting and Exhibit, 8-11 January 2001, Reno, NV, Paper 2001-0648.

10. Corliss, William R., "Propulsion Systems for Space Flight," McGraw-Hill Book Company, 1960.
11. (a) Vinson, John, "Aerospike engine design gains new thrust," Aerospace America, February 1998, pp.30-33.
See also: (b) Weegar, Richard, "Understanding External Expansion Engines," Launchspace Magazine, August 1996, p. 1719.
12. McBride, Bonnie J., and Gordon, Sanford, "Computer program for calculation of complex chemical equilibrium compositions and applications, II. Users manual and program description," NASA Reference Publication 1311, Lewis Research Center, Cleveland, OH 44135, June 1996.
13. Shapiro, Ascher H., "The Dynamics and Thermodynamics of Compressible Fluid Flow, Volume 1," Ronald Press, New York, N. Y., copyright 1953, page 625.

Table 1. Normalized absorption volume for air at 1.18 kg/m^3 as a function of internal energy and laser energy.

u MJ/kg	V_{abs}/β , normalized absorption volume, cm^3					
	$E_L=50 \text{ J}$	$E_L=100 \text{ J}$	$E_L=150 \text{ J}$	$E_L=200 \text{ J}$	$E_L=300 \text{ J}$	$E_L=400 \text{ J}$
1	42.3	84.7	127.1	169.4	254.2	338.9
2	21.1	42.3	63.5	84.7	127.1	169.4
3	14.1	28.2	42.3	56.5	84.7	112.9
4	10.5	21.1	31.7	42.3	63.5	84.7
5	8.47	16.9	25.4	33.9	50.8	67.8
6	7.06	14.1	21.1	28.2	42.3	56.5
7	6.05	12.1	18.1	24.2	36.3	48.4
8	5.30	10.5	15.8	21.1	31.7	42.3
9	4.71	9.42	14.1	18.8	28.2	37.6
10	4.24	8.47	12.7	16.9	25.4	33.9
15	2.82	5.65	8.47	11.3	16.9	22.6
20	2.12	4.24	6.36	8.47	12.7	16.9
30	1.41	2.82	4.24	5.65	8.47	11.3
40	1.06	2.12	3.18	4.24	6.36	8.47
50	0.85	1.69	2.54	3.39	5.08	6.78
60	0.71	1.41	2.12	2.82	4.24	5.65
70	0.61	1.21	1.82	2.42	3.63	4.84
80	0.53	1.06	1.59	2.12	3.18	4.24
90	0.47	0.94	1.41	1.88	2.82	3.77
100	0.42	0.85	1.27	1.69	2.54	3.39
110	0.39	0.77	1.16	1.54	2.31	3.08

Table 2. Measured and calculated quantities for expansion of laser heated STP air.

Quantity	tight focus	loose focus
<u>Measured Quantities</u>		
C (Ns/MJ)	100	150
E_L (J)	300	150
I (Ns)	0.030	0.022
<u>Calculated Quantities with $(\alpha\Phi)_{\max} = 0.25$</u>		
V_{abs} (cm ³)	5.08	5.59
$m_p = \rho_c V_{\text{abs}}$ (mg)	6.00	6.60
$\langle v_e \rangle = I/m_p$ (km/s)	5.00	3.33
$\beta_{\min} = C \langle v_e \rangle / 2(\alpha\Phi)_{\max}$	1.00	1.00
$C^*_{\max} = C/\beta$ (Ns/MJ)	100	150
$(u_c - u^0)_{\min} = \beta E_L / m_p$ (MJ/kg)	50	22.7
T_{\min} see Table 3 (K)	14400	8700
V_{abs} (cm ³)	6.78	6.78
$m_p = \rho_c V_{\text{abs}}$ (mg)	8.00	8.00
$\langle v_e \rangle = I/m_p$ (km/s)	3.75	2.81
$\beta_{\min} = C \langle v_e \rangle / 2(\alpha\Phi)_{\max}$	0.76	0.84
$C^*_{\max} = C/\beta$ (Ns/MJ)	131	178
$(u_c - u^0)_{\min} = \beta E_L / m_p$ (MJ/kg)	28.5	15.7
T_{\min} see Table 3 (K)	9500	7500
V_{abs} (cm ³)	13.6	13.6
$m_p = \rho_c V_{\text{abs}}$ (mg)	16	16
$\langle v_e \rangle = I/m_p$ (km/s)	1.8	1.4
$\beta_{\min} = C \langle v_e \rangle / 2(\alpha\Phi)_{\max}$	0.38	0.42
$C^*_{\max} = C/\beta$ (Ns/MJ)	262	356
$(u_c - u^0)_{\min} = \beta E_L / m_p$ (MJ/kg)	14.3	7.9
T_{\min} see Table 3 (K)	7000	5400

← New
Table

Table 3. Thermodynamic properties of equilibrium air; $\rho = 1.18 \text{ kg/m}^3$.

u	T	P	h	s	c_p	M_m	$X(e^-)$	v_a	c_p/c_v
MJ/kg	10^3 K	bar	MJ/kg	KJ/kg K	KJ/kg K	kg/kmol		km/s	
-0.9	0.298	1.000	-0.004	6.864	1.005	28.965	0	0.346	1.40
1	1.6	5.4	1.5	8.2	1.25	29.0	4E-10	0.77	1.30
2	2.5	8.6	2.7	8.7	1.51	28.9	3.E-09	0.95	1.24
3	3.2	11.1	3.9	9.0	2.16	28.6	3.E-08	1.06	1.20
4	3.7	13.1	5.1	9.3	2.83	27.8	3.E-07	1.15	1.19
5	4.1	15.0	6.3	9.6	3.15	26.9	2.E-06	1.23	1.19
6	4.5	16.9	7.4	9.8	3.04	26.1	5.E-06	1.32	1.21
7	4.9	19.1	8.6	10.0	2.69	25.3	2.E-05	1.41	1.23
8	5.4	21.5	9.8	10.2	2.56	24.7	4.E-05	1.50	1.23
9	5.9	23.9	11.0	10.4	2.86	24.2	8.E-05	1.57	1.21
10	6.3	26.0	12.2	10.6	3.43	23.8	1.E-04	1.62	1.19
15	7.5	34.1	17.9	11.3	6.70	21.7	5.E-04	1.84	1.17
20	8.3	41.3	23.5	11.9	8.93	19.8	9.E-04	2.02	1.17
30	9.7	56.2	34.8	13.0	9.09	16.9	3.E-03	2.38	1.19
40	11.5	75.4	46.4	14.0	5.13	15.0	1.E-02	2.81	1.24
50	14.4	101.0	58.5	14.8	4.81	14.0	4.E-02	3.26	1.25
60	16.6	124.0	70.5	15.4	6.62	13.2	1.E-01	3.60	1.24
70	18.4	145.0	82.3	16.0	8.25	12.4	1.E-01	3.91	1.24
80	19.9	167.0	94.1	16.5	9.51	11.7	2.E-01	4.20	1.24
90	21.3	189.0	106.0	17.0	10.40	11.1	2.E-01	4.48	1.25
100	22.6	211.0	118.0	17.4	10.90	10.5	3.E-01	4.76	1.26
110	23.9	235.0	130.0	17.9	11.10	10.0	3.E-01	5.03	1.27

Table 4. Thermodynamic properties of Mach 5 air at stagnation density, $\rho = 5.90 \text{ kg/m}^3$.

u	T	P	h	s	c_p	M	$X(e^-)$	v_a	c_p/c_v
MJ/kg	10^3 K	bar	MJ/kg	KJ/kg K	KJ/kg K	kg/kmol		km/s	
0.102	0.560	9.492	0.263	6.864	1.042	28.965	0	0.471	1.38
1	1.6	27.1	1.5	7.7	1.25	28.97	4e-13	0.77	1.30
2	2.6	43.2	2.7	8.2	1.45	28.95	6.E-11	0.96	1.25
3	3.3	56.5	4.0	8.6	1.85	28.73	2.E-08	1.08	1.21
4	3.9	67.7	5.1	8.9	2.33	28.19	3.E-07	1.17	1.20
5	4.4	78.2	6.3	9.1	2.65	27.46	2.E-06	1.26	1.20
6	4.8	88.9	7.5	9.3	2.71	26.69	6.E-06	1.35	1.22
7	5.3	100.3	8.7	9.5	2.61	25.96	2.E-05	1.45	1.23
8	5.8	112.4	9.9	9.7	2.55	25.32	4.E-05	1.53	1.23
9	6.3	124.5	11.1	9.9	2.69	24.79	8.E-05	1.61	1.22
10	6.7	135.8	12.3	10.0	3.04	24.32	1.E-04	1.67	1.21
15	8.2	182.0	18.1	10.7	5.49	22.19	6.E-04	1.91	1.18
20	9.2	222.3	23.8	11.2	7.36	20.32	1.E-03	2.11	1.18
30	10.8	304.9	35.2	12.2	8.05	17.41	3.E-03	2.49	1.20
40	12.7	404.9	46.9	13.1	5.52	15.45	1.E-02	2.92	1.24
50	15.6	534.8	59.1	13.8	4.28	14.33	3.E-02	3.39	1.27
60	18.4	667.9	71.3	14.4	5.20	13.54	8.E-02	3.78	1.26
70	20.8	794.6	83.5	14.9	6.32	12.81	1.E-01	4.13	1.27
80	22.8	919.9	95.6	15.4	7.26	12.14	2.E-01	4.45	1.27
90	24.6	1046.6	107.7	15.8	7.99	11.52	2.E-01	4.76	1.28

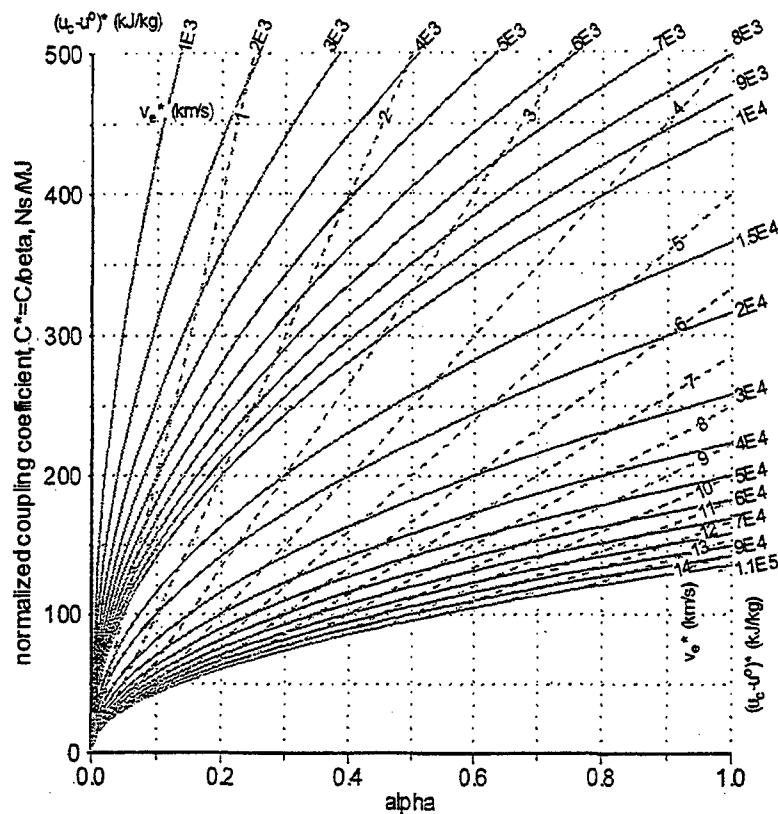


Figure 1. Defined relationships between six variables of interest: C^* , α , β , Φ , $\langle v_e \rangle^*$, and $[u_c - u^o]^*$. The plots show $C^* = C/\beta$ as a function of α , with lines of constant $v_e^* = \langle v_e \rangle^* / \Phi$ and constant $[u_c - u^o]^* = [u_c - u^o]^* / \Phi$. The plots may alternatively be interpreted as a C vs α plots with lines of constant $v_e^* = \langle v_e \rangle^* / \beta \Phi$ and constant $[u_c - u^o]^* = [u_c - u^o]^* / \beta^2 \Phi$.

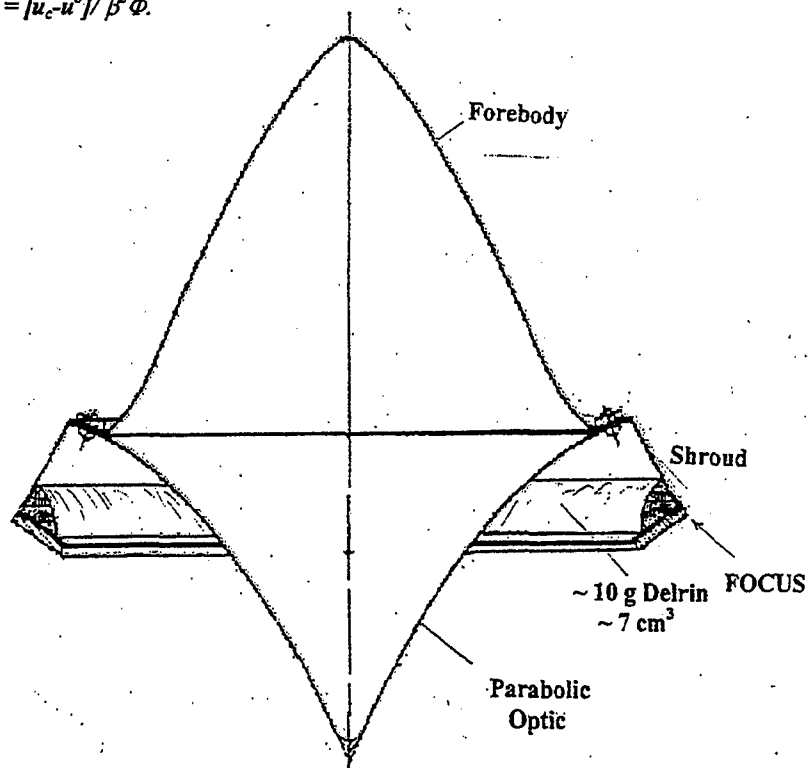


Figure 2. Cross-sectional view of Myrabo Laser Lightcraft, Model 200-3/4. The maximum diameter of the test article at the shroud is ~ 10 cm. The indicated ring of Delrin weighs ~ 10 g and has a volume of ~ 7 cm^3 and a surface area ~ 25 cm^2 . The idealized maximum plug nozzle exit area is ~ 350 cm^2 .

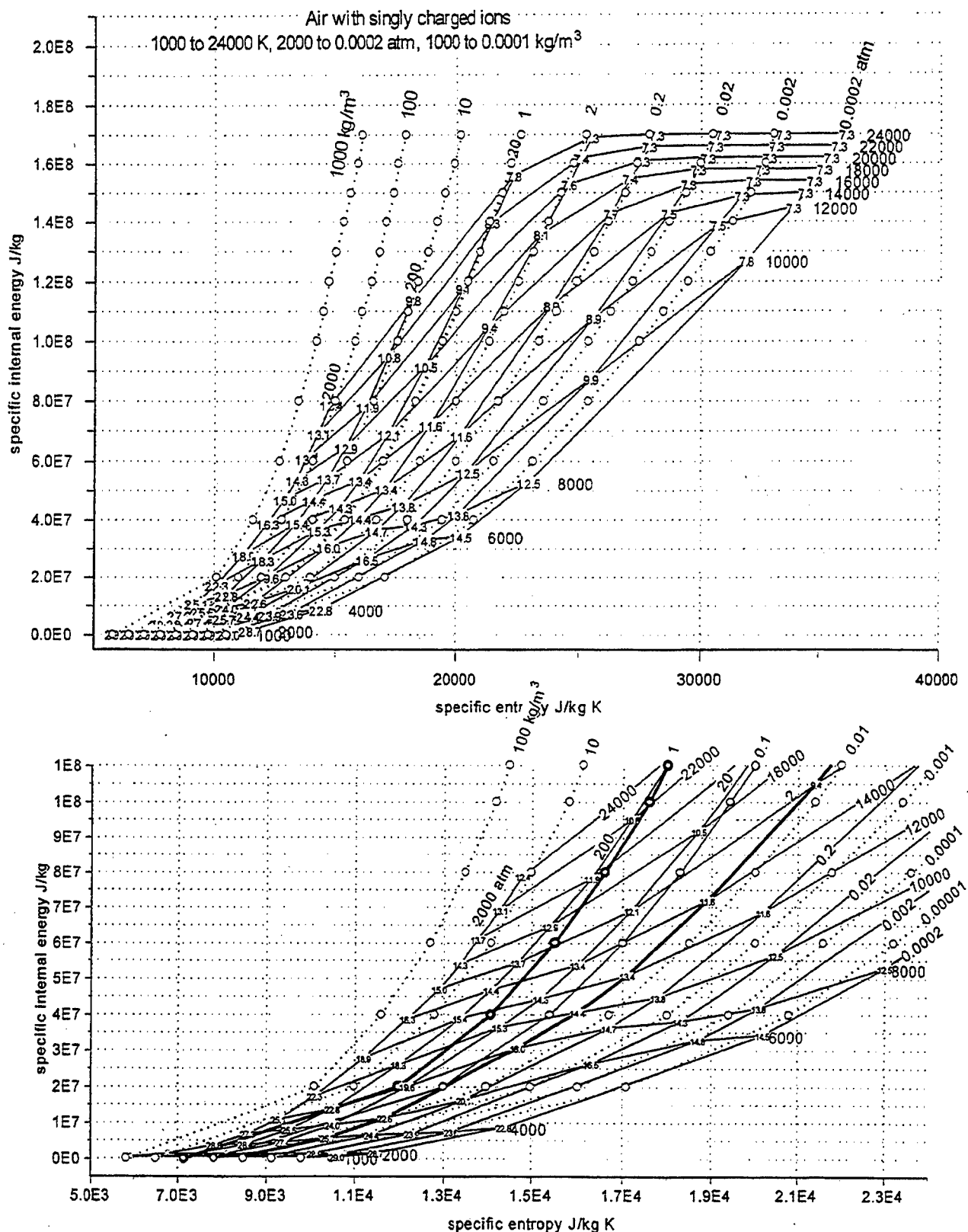


Figure 3. Mollier diagram for air including singly ionized species. Molecular weights are indicated at intersections of isobars and isotherms. The lower diagram shows a heavy constant density line, $\rho = 1.18 \text{ kg/m}^3$ above a heavy constant pressure line, $P = 1 \text{ atm}$. The maximum energy initial states of laser heated STP air lie on the constant density line and the optimally expanded states lie vertically below on the constant pressure line.

